STRAIN INDUCED PHASE TRANSFORMATION FROM MARTENSITIC TO AUSTENITIC PHASES BY NITROGEN SOLID SOLUTION

Abdelrahman Farghali[1], Tatsuhiko Aizawa[2]

[1]Graduate School of Material Science and Engineering, Shibaura Institute of Technology

[2]Department of Engineering and Design, Shibaura Institute of Technology

[1]abdelrahman_mohamed@eng.suez.edu.eg, [2]taizawa@sic.shibaura-it.ac.jp

ABSTRACT

An investigation on phase transformation of austenitic stainless steel was carried out on AISI 304 stainless steel with a large amount of nitrogen. A plasma nitriding process was performed on the stainless steel at lower temperatures to increase the nitrogen content up to 10 mass percent. In this study low temperature plasma nitriding was applied at a holding temperature lower than 700K to avoid any synthesized precipitates such as chromium nitride by nitrogen solid solution. This high concentration of nitrogen interstitial solutes into the super-cells of stainless steel resulted in occupation of the octahedral or tetrahedral vacancies and in anisotropic lattice expansion in the c axis. This expansion accompanied with significant straining of crystalline structure in α'-phase. In the inverse manner to the phase transformation from γ-phase to α'-phase under compression, the transformation took place from the martensitic phase to austenitic phase. XRD and SEM/EDX were utilized to describe the high nitrogen concentration by the low temperature plasma nitriding and the inverse phase transformation.

1. INTRODUCTION

Manufacturing with severe straining often accompanies with grain size refinement and phase transformation. For an example, the shear straining during the micro-piercing process for austenitic stainless steel AISI304 sheet acts as a driving force to initiate the martensitic phase transformation along the pierced holes together with grain refinement and crystalline orientation change(Shiratori, 2015). The fcc-structured austenitic stainless steel sheet shears at the <110> directions with the transformation to a bct crystal structure. By applying the compressive strains in the c axis, this bct structure shrinks in the c-axis together with elongation along the a-axis. Then, this bct structure transforms into the bcc martensitic crystal structure. This phenomenon is called the transformation induced plasticity (TRIP) (Tamura, 1982).

The plasma nitriding (PN) process is classified into two categories; high temperature (HT) plasma nitriding and low temperature (LT)-PN (Anzai, et al., 2011; Santoyoyo, 2014; Aizawa, 2015).In case of stainless steels, the critical border between HT-PN and LT-PN is function in the holding temperature and the nitriding duration time. Under short-term nitriding conditions, where the present study is concerned, PN with the higher temperature than 723 K is classified as HT-PN where chromium nitrides are mainly synthesized as a precipitate for hardening. Besides for the precipitation reaction to synthesize the nitrides, there is no difference in the detected XRD diagrams before and after HT-PN. That is, the nitrogen solute content in the HT-PN stainless steels is nearly equal to the maximum nitrogen solid solubility of stainless steels (Granito, et al., 2002).

On the other hand, no nitrides are detected in XRD diagrams in case of LT-PN under the lower holding temperature than 723 K. In fact, when plasma-nitriding the AISI316 and AISI304 stainless steels at 673 K, no CrN are synthesized (Anzai, 2011). Instead of the precipitation reaction, the peak for austenite phase before PN significantly shifts to the lower angel side. That is, this LT-PN accompanies with the γ-lattice expansion. This intrinsic straining results in solid solution hardening in the plasma nitrided austenitic stainless steels.

Through our previous studies (Aizawa, et al., 2015), the above LT-PN behavior is observed and distinguished even in the case of martensitic stainless steels such as AISI420 and AISI420-J2 substrates. That is, 1) no formation of nitrides 2) α'-lattice expansion 3) solid-solution hardening. A significant difference in LT-PN between the austenitic and martensitic stainless steels lies in the possible phase transformation; i.e. α'-

phase (or bcc-structure) to γ-phase (or fcc-structure).

In the present study, XRD, EDX and XPS analyses are performed to investigate this possibility of α' to γ-phase transformation by higher nitrogen solid solution. First, the high density plasma nitriding system is introduced with comments on the characteristics of present nitriding system. XRD/XRF is utilized to make structural analysis. SEM-EDX is used for microstructural analysis and nitrogen mapping. XPS is also employed to describe the chemical shift in the nitrogen solid solution state with high concentration. On the basis of these analyses, a theoretical model of phase transformation by nitrogen solute concentration is proposed.

2. EXPERIMENTAL PROCEDURE

2.1 Plasma Nitriding System

As illustrated in Fig. 1, being different from the DC- or RF-plasma generators, where the plasmas are ignited and generated in the frequency of 13.56 MHz or its multiples, the present high density nitriding system has no mechanical matching box with slow response time of 1 s to 10 s to adjust the applied power. Since both the input and output powers are automatically matched by frequency adjustment around 2 MHz, the matching response time is only limited to 1 ms at most. This prompt power control provides to make full use of mesoscopic plasma pressure range over 50 Pa. Different from the conventional processes, the vacuum chamber is electrically neutral so that RF-power and DC-bias should be controlled independently from each other. A dipole electrode is utilized to generate RF-plasma; DC bias is directly applied to the specimens. Heating unit is located under this DC-biased cathode plate.

In the following nitriding experiments, the specimens are located on the cathode table before evacuation down to the base pressure of 0.1 Pa. Then, nitrogen gas is first introduced as a carrier gas for heating. After heating to the specified holding temperature, the nitrogen pre-sputtering is started at the constant pressure. After pre-sputtering, the hydrogen gas is added to nitrogen gas with the specified partial pressure ratio.

2.2 Specimens

AISI-SUS420 specimens were prepared for description of plasma nitriding behavior. A square sample with 25 x 25 x 5 mm^3 as well as a circular disc specimen with the diameter of 25 mm and the thickness of 5 mm were commonly used to make XRD and SEM-EDX analyses and to measure the hardness depth profile in the nitrided specimen.

2.3 Observation and Measurement

Optical microscope, SEM (Scanning Electron Microscope) and EDX (Energy Dispersive X-ray spectroscopy) are utilized to describe the microstructure and element distribution in the cross-section of plasma nitrided specimens. XRD (X-Ray Diffraction) and XRF (X-Ray Fluorescence)is used to analyze the phase change by the low temperature plasma nitriding.

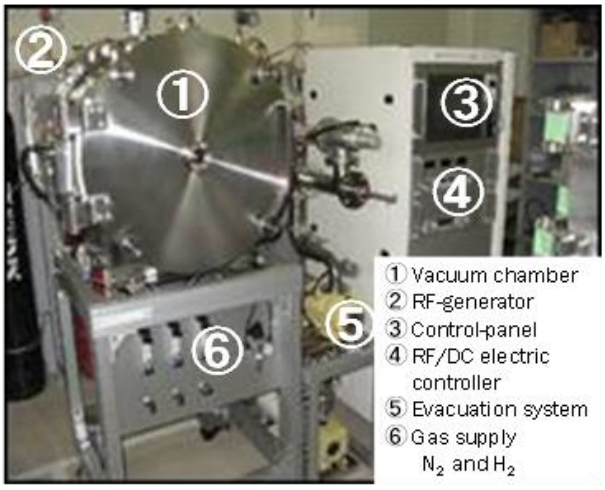

Fig. 1 High density plasma nitriding system working in the low temperature.

3. RESULTS AND DISCUSSION

3.1 Nitrogen Solid Solution

The nitrided AISI420 specimen at 673 K for 14.4 ks was halved by wire-cutting to investigate the microstructure and nitrogen solute map on its cross-section. SEM and EDX were utilized to describe the nitrogen concentration in the depth of nitrided layer.

Figure 2 depicts the depth profiles of constituent chromium and diffusing nitrogen contents, measured by EDX. At the vicinity of surface, the nitrogen solute content becomes 9 mass% in average. The maximum solid solubility of nitrogen into irons was only 0.1 mass% after the phase diagram of Fe-N system (JIM, 1974). The highest surface nitrogen contents of plasma nitrided tool steels and stainless steels by using the commercial process at 823 K was reported to be 0.1 to 0.2 mass% (Hirooka, 2010). This high surface nitrogen content significantly characterizes the present inner nitriding process at low temperature.

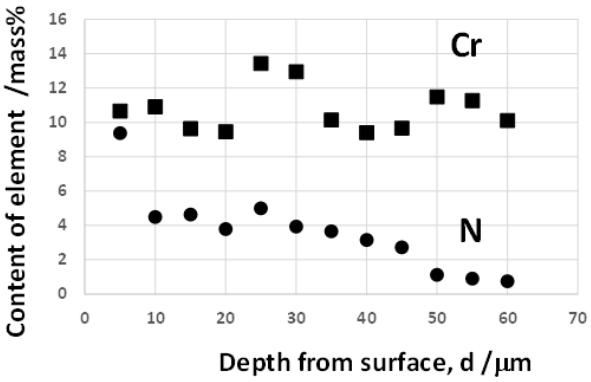

Fig. 2: Chromium and nitrogen depth profile across the nitrided layer from the surface, analyzed by SEM/EDX with the incremental positioning of 5 μm.

The nitrogen content decreases from this high concentration at the surface down to 4 mass % in the middle range of thickness and goes to nearly zero near the nitriding front end. In particular, the plateau with constant nitrogen content around 4 mass % is formed in the range of 10 to 40 μm in depth. As analyzed by (Hirooka, 2010, Granito, 2002), since every inner nitriding process in the high temperature plasma nitriding is governed by the nitrogen diffusion mechanism, the nitrogen content exponentially decreases from the surface to the depth toward the nitriding front end. This nitrogen content depth profile in the nitrided stainless steels is intrinsic to the present low temperature plasma nitriding.

On the other hand, little change is detected in the chromium concentration along the depth of nitrided layer. In fact, the average of chromium content is 12 mass %, which is the same as the initial content of AISI420 stainless steels, with the deviation of 1.5 mass %, as shown in Fig. 2. This implies that no chromium is used for precipitation reaction of CrN during plasma nitriding. Remembering that large amount of chromium constituents in the matrix is used to form a compound (Hirooka, et al., 2010, Granito, et al., 2002), the thermal and corrosion resistance, intrinsic to original stainless steels, must be never lost even after the present plasma nitriding.

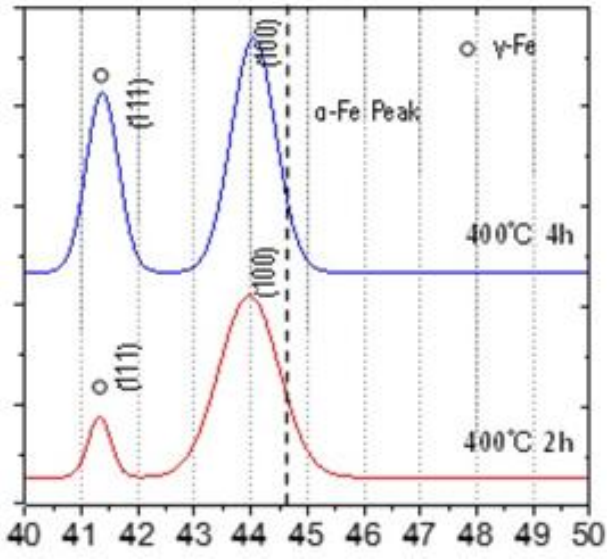

Fig. 3 XRD diagrams of plasma nitrided specimens at 673 K (or 400 ^{o}C) for 7.2 and 14.4 ks.

XRD analysis was also performed to investigate whether the nitride precipitates were synthesized by plasma nitriding at 693 K for 7.2 ks and 14.4 ks. Figure 3 depicts the XRD diagram; no nitride peaks are detected. That is, no nitride precipitates are synthesized during this plasma nitriding. The original diffraction peak for (100) plain for AISI420 stainless steels is located at $2\theta = 44.7^{o}$ before nitriding. On the other hand, the detected of (100) plain for α'-Fe peak of nitrided specimen at 673 K both for 7.2 ks and 14.4 ks in Fig. 3 shifts to the lower 2θ side; e.g., the peak of (100) plain in the α'-Fe shifts in Fig. 3 from $2\theta = 44.7^{o}$ to $2\theta = 44^{o}$ after nitriding. This implies that the original α-Fe crystalline cell expands by nitrogen solid solution.

In parallel with this lattice expansion, another peak is detected at $2\theta = 41.3^{o}$in Fig. 3 for the nitrided specimens for 7.2 ks and 14.4 ks, respectively. After (Anzai, 2011), this peak must be a diffraction peak for (111) of fcc-structured stainless steel or γ-phase. This peak intensity is enhanced with increasing the duration time from 7.2 ks to 14.4 ks in plasma nitriding. After EDX analyses of these two specimens, the nitrogen content at the surface is more than 4 mass% for both specimens. This implies that higher nitrogen concentration at the surface with increasing the nitriding time drives this phase transformation.

3.2 Nitrogen Occupation to Vacancy Sites

Owing to the first principle calculation on the interstitial behavior of nitrogen into α-Fe in (Domain, 2004), the above peak shift is driven by occupation of nitrogen solutes into vacancy sites. The above site occupation of vacancies by nitrogen interstitials advances with straining into the super-lattice. This strain results in the elongation of α'-Fe super-lattice in its c-axis direction. Although few experimental studies were reported on the α'-Fe lattice expansion by nitrogen interstitial process, a significant peak shifts was experimentally detected for various martensitic Fe-Cr alloys in common after nitrogen ion implantation in (Manova,2006) even at lower temperature than 673 K. Most of measured XRD diagrams indicated that α'-Fe peak shifted from 44.7^{o} to 44^{o}; the average strain induced in the c-axis direction by interstitial site occupation in α'-Fe lattice was reported to be 3 to 5 %. These results correspond to the peak shift of (100) plain of α'-Fe in Fig. 3.

3.3 Theoretical Model

In the above theoretical and experimental studies on the lattice expansion as well as straining of α'-Fe by nitrogen interstitial site occupation, no direct statements were reported on the phase transformation from α'-Fe to γ-Fe. Owing to the discussion in (Domain, 2004), the gradual increase of N/(N+Fe) atomic ratio in the super-cell of α'-Fe might result in the selective site occupation of vacancies in the α'-Fe supercell. First and second nitrogen interstitial nitrogen solutes are allowed to be present by their occupation of one octahedral vacancy and one tetrahedral vacancy in α'-Fe supercell. This asymmetric occupation process induces the shear strain into the lattices as well as normal strain in the c-axis. If this occupation could advance further in the α'-Fe supercell by more increase of N/(N+Fe) ratio, more strains could be stored in the current α'-Fe supercell with sufficient amount to induce the transformation by minimization of strains in it.

Let us consider the possible model for phase transformation from α'-phase (or bcc-structure) to

γ-phase (or fcc-structure) by high nitrogen concentration in the following.

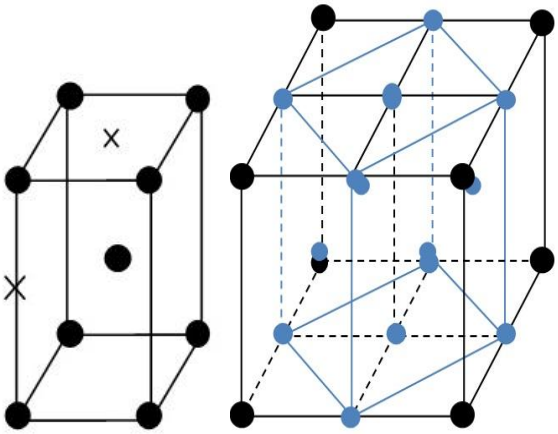

Fig. 4Phase transformation induced by high nitrogen concentration through the occupation into vacancy sites. (a)Position of nitrogen atoms × inside the bct lattice (b) Four martensitic bct lattice transforms into one austenite fcc lattice.

The high nitrogen concentration inside the α'-Fe cell induces the normal anisotropic straining in the <001> and <110> directions. This leads to an expansion and contraction in the c-axis and a-axis of α'-Fe cell, respectively. The axial ratio of lattice constants or c/a, increases itself with higher nitrogen content up to 10 mass% (c/a ≈ 1.375)(IMAI, 1965).A phase transformation from bcc to bct occurs together with nitrogen atoms occupation into the octahedral and tetrahedral sites as shown in Fig. 4 (a). The expanded bcc-structured α'-Fe cells tends to be close to the bct-structures by storing the high strain energy inside. This transient crystalline structure is easy to transform into a lower energy state. That is, four bct unit cells generates a single fcc austenite lattice as shown in Fig 4 (b). This transformation model by high tensile straining with asymmetric site occupation of nitrogen interstitials into vacancy sites in α'-Fe lattices is just inverse to the transformation mechanism from γ-phase to α'-phase by compressive straining.

CONCLUSION

High nitrogen concentration as an interstitial solute tothe α'-Fe cell of martensitic stainless steels drives the anisotropic lattice expansion together with highly strained state. The expanded crystalline structure turns to be close to the transient bct-structure with increasing the nitrogen content. In the relaxing process from these transient states in the bct structure to more stable crystalline state by releasing the stored strain energy, the transformation takes place from bct to fcc-structured stainless steels. Further experimental theoretical works are planned to demonstrate this modeling in near future.

ACKNOWLEDGEMENTS

The authors would like to express their gratitude to Ms. K. Hashimoto, Dr. K. Wasa (Tec. Dia., Co. Ltd.), and, Mr. T. Shiratori (Komatsu Precision, Co. Ltd.) for their help in measurement. This study is financially supported by the ABE-Initiative Project, Japan Government.

REFERENCES

Aizawa, T., Katoh, H., 2015, Low temperature plasma nitriding process in the stainless steels, Proc. 9th SEATUC Conference (Thai) CD-ROM.

Anzai, H., (Ed.), 2011, Surface treatment for high qualification of dies and molds, Nikkan-Kougyou.

Domain, C., et al., 2004, Ab initio study of foreign interstitial atom (C, N) interactions with intrinsic point defects in α-Fe. Physical Review B69, 114112.

Granito, N., Kuwahara, H., Aizawa, T., 2002, J. Materials Science. 37, pp. 835-844

Hiroka, Y., Inoue, K., 2010, Denki-Seiko 80-1 (2010) 15-24..

Imai, Y., Izumiyama, M., Tsuchiya, M., 1965, Thermodynamic study on the transformation of austenite into martensite in iron-high nitrogen and iron-carbon binary system, the res. Inst. Tohuku Univ., A17, 173.

Japan Institute of Metals (JIM) (ed.), 1974, Metals Data Book, Maruzen, Tokyo, 25.

Manova, D., et al., 2006, Variable lattice expansion in martensitic stainless steel after nitrogen ion implantation," Nucl. Inst. Meth. Phys. Res. B 242, 285-288.

Santoyoyo, D., Aizawa, T., Shinji, M., Morita, H., 2014, Micro-texturing of stainless steels via high density plasma nitriding, Proc, 8th ICOMM, 90, pp. 1-8.

Shiratori, T., et al., 2015, Effects of fine-grained micro-structure on process effected zone in micro-piercing of austenitic stainless steel SUS304, Proc. 8th AWMFT (Suwa) CD-ROM.

Abdelrahman Farghali received the B.E. (2013) degrees in the Mechanical Engineering from Suez Canal University. He is a preliminary graduate student, School of Engineering and Science, SIT. His Current interests include manufacturing science.

Tatsuhiko Aizawa received the B.E. (1975), M.E. (1977), and D.E. (1980) degrees in the Nuclear Engineering from the University .of Tokyo. He is a Professor, Department of Engineering and Design, Shibaura Institute of Technology. His Current interests include micro-manufacturing, innovations in manufacturing and materials processing, and, materials science and engineering.